Fabrication error analysis and experimental demonstration for computer-generated holograms

Ping Zhou, Jim Burge

College of Optical Sciences, University of Arizona, Tucson, AZ, 85721

Aspheric optical surfaces are often tested using computer-generated holograms (CGHs). For precise measurement, the wavefront errors caused by the CGH must be known and characterized. A parametric model relating the wavefront errors to the CGH fabrication errors is introduced. Methods are discussed for measuring the fabrication errors in the CGH substrate, duty-cycle, etching depth and effect of surface roughness. An example analysis of the wavefront errors from fabrication non-uniformities for a phase CGH is given. The calibration of these effects for a CGH null corrector is demonstrated to cause measurement error less than 1nm.

© 2006 Optical Society of America

OCIS codes: 050.1380, 090.2880, 120.2880

1. Introduction

Optical elements with large aspheric departures are often tested with the help of computer-generated holograms.[1-3] The primary role of CGHs is to generate reference wavefronts of any desired shape. An accurately drawn pattern on the CGH provides accurate wavefront control. The precision of the CGH pattern affects the accuracy and validity of the measurement results. The CGH errors can be design errors, alignment errors or fabrication errors. The surface measurement can suffer from all these errors. The CGH design errors and alignment errors are discussed elsewhere.[4,5] In this paper, we only focus on how the CGH fabrication errors affect the wavefront performance.

The CGH fabrication errors can be classified into five types:

- Substrate figure errors: substrate surface variation from its ideal shape
- Pattern distortion errors: displacement of recorded pattern from its ideal position
- Duty-cycle errors: variation in duty-cycle
- Etching depth errors: variation in etching depth
- Surface roughness errors: variation in surface roughness

The effects of all these fabrication errors are coupled together, and it is difficult to decouple the individual effects of each error source on the wavefront. Chang and Burge first developed a parametric model to relate the fabrication errors to the wavefront performance.[6,7] This model is summarized and extended in this paper. This parametric model can help estimate wavefront measurement errors due to a CGH in optical testing. Some methods to determine the fabrication non-uniformities in the duty-cycle, etching depth and surface roughness are provided in section 3. A wavefront error analysis for a phase CGH is shown in section 4. The calibration of CGH substrate is demonstrated in section 5 to provide measurement accurate to about 1nm rms.

2. Parametric model

The binary, linear grating model is used to build the parametric model based on scalar diffraction theory. The scalar theory assumes that the wavelength of the incident light is much smaller than the grating period S. Only the far-field diffraction effects will be of interest. Furthermore, it is assumed that the grating is illuminated with a planar wavefront at normal incidence. Fig.1 illustrates a binary, linear grating.

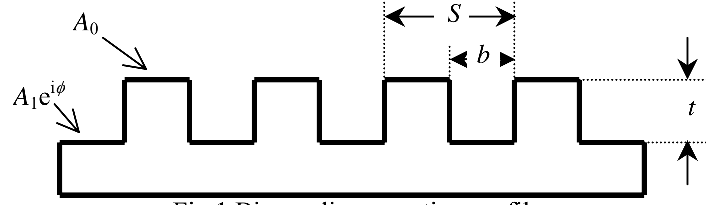

Fig.1 Binary, linear grating profile

The grating is defined by the period S and the etching depth t. Duty-cycle is defined as $D = b / S$, where b is width of the etched area. A_0 and A_1 correspond to the amplitudes of the output wavefront from the unetched area and etched area of the grating, respectively. The phase function ϕ represents the phase difference between rays from the peaks and rays from the valleys of the grating structure, which equals to $2\pi(n-1)t/\lambda$ for the grating in transmission mode.

The approach of the linear grating model for CGH characterization has already been developed by Chang and Burge. The diffracted wavefront phase is Ψ. The wavefront phase sensitivity functions $\partial\Psi/\partial D$ and $\partial\Psi/\partial\phi$ are introduced to specify the wavefront error caused by small deviations in duty-cycle ΔD and in phase function $\Delta\phi$. Here, the model is extended with the introduction of the wavefront sensitivity function $\partial\Psi/\partial\left(A_0/A_1\right)$, which describes the wavefront error caused by a small deviation of the ratio of two amplitudes, $\Delta(A_0/A_1)$.[8] The deviation of the amplitude ratio is due to local surface roughness variations. Table 1 summarizes the wavefront sensitivity functions and the diffraction efficiencies for the zero and the non-zero diffraction orders.

Table 1. Summary of equations for parametric model analysis

	Zero order ($m = 0$)	Non-zero order (m ±1, ±2,…)
	Diffracted wavefront	
η diffraction efficiency	$A_0^2(1-D)^2 + A_1^2 D^2 + 2A_0A_1D(1-D)\cos(\phi)$	$\left[A_0^2 + A_1^2 - 2A_0A_1\cos(\phi)\right]D^2\,\text{sinc}^2(mD)$
$\tan\left(\Psi\right)$ Ψ : wavefront phase	$\dfrac{A_1D\sin(\phi)}{A_0(1-D)+A_1D\cos(\phi)}$	$\dfrac{A_1\sin(\phi)\cdot\text{sinc}(mD)}{[-A_0+A_1\cos(\phi)]\cdot\text{sinc}(mD)}$
	Sensitivity functions	
$\dfrac{\partial\eta}{\partial D}$	$-2A_0^2(1-D)+2A_1^2D+2A_0A_1(1-2D)\cos\phi$	$2\left[A_0^2+A_1^2-2A_0A_1\cos(\phi)\right]D\,\text{sinc}(2mD)$
$\dfrac{\partial\eta}{\partial\phi}$	$-2A_0A_1D\left(1-D\right)\sin\phi$	$2A_0A_1\sin\phi\,D^2\,\text{sinc}^2\left(mD\right)$
$\dfrac{\partial\Psi}{\partial D}$	$\dfrac{A_0A_1\sin\phi}{A_1^2D^2+A_0^2(1-D)^2+2A_0A_1D(1-D)\cos\phi}$	$\begin{cases}\infty, & \text{for } \text{sinc}(mD)=0\\ 0, & \text{otherwise}\end{cases}$
$\dfrac{\partial\Psi}{\partial\phi}$	$\dfrac{A_1^2D^2+A_0A_1D(1-D)\cos\phi}{A_1^2D^2+A_0^2(1-D)^2+2A_0A_1D(1-D)\cos\phi}$	$\dfrac{A_1^2-A_0A_1\cos\phi}{A_1^2+A_0^2-2A_0A_1\cos\phi}$
$\dfrac{\partial\Psi}{\partial(A_0/A_1)}$	$\dfrac{-D(1-D)\cdot\sin\phi}{(A_0/A_1)^2(1-D)^2+D^2+2D(1-D)(A_0/A_1)\cos\phi}$	$\dfrac{\sin\phi}{(A_0/A_1)^2+1-2(A_0/A_1)\cos\phi}$

The sensitivity functions can be evaluated directly to give the wavefront error due to variations in duty-cycle D, etch depth t or amplitude ratio A_0/A_1. These functions are shown in Eqs.1-3 respectively,

$$\Delta W_D = \frac{1}{2\pi}\frac{\partial \Psi}{\partial D}\cdot \Delta D = \frac{1}{2\pi}\frac{\partial \Psi}{\partial D}\cdot\left(\frac{\Delta D}{D}\right)\cdot D\,, \tag{1}$$

$$\Delta W_\phi = \frac{\partial \Psi}{\partial \phi}\cdot \Delta\phi = \frac{\partial \Psi}{\partial \phi}\cdot\left(\frac{\Delta \phi}{\phi}\right)\cdot \phi\,, \tag{2}$$

$$\Delta W_{A_0/A_1} = \frac{1}{2\pi}\frac{\partial \Psi}{\partial \left(A_0/A_1\right)}\cdot \Delta\left(\frac{A_0}{A_1}\right), \tag{3}$$

where

ΔD : duty-cycle variation across the grating,

ΔW_D : wavefront variation in waves due to duty-cycle variation,

$\Delta\phi$: etching depth variation in radians across the grating,

ΔW_ϕ : wavefront variation in waves due to etching depth variation,

$\Delta(A_0/A_1)$: variation of the ratio of A_0 to A_1,

$\Delta W_{A_0/A_1}$: wavefront variation in waves due to amplitude variation.

As long as the duty-cycle, etching depth and amplitude vary over spatial scales that are large compared to the grating spacing, the equations 1 to 3 can be used to determine the coupling between fabrication errors and system performance. The wavefront sensitivity functions provide a means of calculating the wavefront phase changes that result from the fabrication non-uniformities. They can be used to identify which hologram structures are the most or the least sensitive to those fabrication uncertainties. The information may also be used to estimate error budgets for applications using the CGHs.

Note that the wavefront phase change caused by a constant fabrication error in duty-cycle, etching depth or amplitude ratio can not be measured. This is because the constant phase change is regarded as piston and it is often removed in optical testing. This parametric model relates the wavefront errors to the fabrication non-uniformities. The wavefront error can be estimated if the fabrication non-uniformities in duty-cycle, etching depth and amplitudes are known.

Another wavefront error is from CGH pattern position. Pattern position error, also called pattern distortion, means the recorded pattern in a CGH is displaced from its ideal position. The amount of wavefront errors produced by the CGH pattern distortions can be expressed as

$$\Delta W(x,y) = -m\lambda\frac{\varepsilon}{S}\,, \tag{4}$$

where ε is the grating position error in the direction perpendicular to the pattern. The produced wavefront phase errors due to pattern distortions are linearly proportional to the diffraction order number and inversely proportional to the local fringe spacing.[9] CGH pattern distortion errors do not affect the zero-order diffracted beam. Pattern distortion can be measured with a microdensitometer or using an interferometric method.[10,11]

3. Measurement of fabrication errors

In order to quantify the wavefront error in optical testing, the fabrication non-uniformities for each error source must be determined. These fabrication non-uniformities can be obtained by measuring a set of sampled points over the CGH.

3.1 Substrate measurement

Substrate errors are typically of low spatial frequencies. Their effects on the wavefront depend on the applications of the CGH. If the CGH is used in reflection, a surface defect on a CGH substrate with a peak-to-valley deviation of δs, where s refers to the ideal surface figure, will produce a wavefront error of $2\delta s$. A transmission CGH that has the same peak-to-valley surface defect, on the other hand, will produce a wavefront phase error of $(n\text{-}1)\delta s$, where n is the index of refraction of the substrate. The substrate errors influence all the diffraction orders equally.[12]

One method of eliminating substrate errors in a CGH is to measure the flatness of the substrate before the grating patterns are written. This procedure can be done on a Fizeau interferometer. Another method is to measure the effect of surface irregularities using the zero order diffraction from the CGH, and subtract this from the non-zero-order surface measurement. A test setup is illustrated in Fig.2, where the CGH is placed in a diverging beam instead of a collimated beam, because that is the actual working configuration for this CGH. The reference sphere is first measured, then the wavefront with the CGH is tested. The difference of these two measurements depicts the transmitted wavefront error of the CGH in zero order diffraction, which is mainly CGH substrate error.

Note that besides the CGH substrate error, the wavefront errors introduced by the non-uniformities in duty-cycle, etching depth, and amplitude ratio also affect the zero-order measurement. These errors affect to zero and non-zero orders differently. When we subtract the non-zero-order surface measurement from the zero-order measurement, the CGH substrate error can be totally removed, leaving the residual wavefront errors from the fabrication non-uniformities.

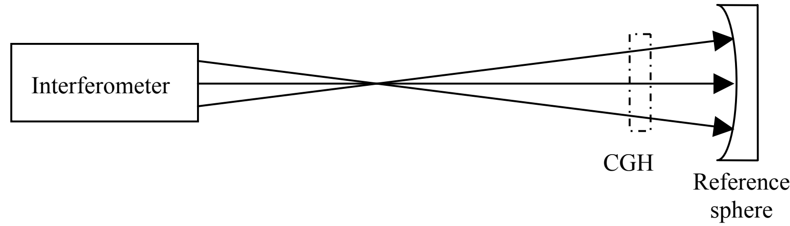

Fig.2 Setup of CGH substrate measurement

3.2 Duty-cycle and etching depth measurement

Variations in duty-cycle and etching depth can be measured using either an atomic force microscope (AFM) or an interference microscope, which provide the surface relief of the CGH. Another method is to measure the diffraction efficiencies of several diffraction orders, and then fit the duty-cycle and etching depth. A set of the sampled points should be measured to obtain the variations in duty-cycle and etching depth. The duty-cycle and etching depth at each sampled point are determined by using the nonlinear least square fit. The CGH is illuminated with a finite small laser spot, so the fitted results are the average duty-cycle and etching depth over that illuminated area.

To verify the feasibility of the second method, a Monte Carlo analysis was used to find the relationship between the number of diffraction orders measured and the accuracy obtainable for the duty-cycle and etching depth. The results shown in Fig.3 are for a 1000-trial Monte Carlo simulation. The nominal duty-cycle and etching depth are 0.49 and 0.33λ respectively in this simulation. These are the measured parameters of a CGH demonstrated in next section. A_0 and A_1 are assumed to be unity, since it is a phase CGH. A uniform-distributed random error is added to each diffraction efficiency measurement. Measurement errors of up to ±1%, ±3% and ±5% for each order are assumed in the analysis. δt and δD are the standard deviations of the etching depth and duty-cycle of the 1000 trials, which represent the measurement confidence level of the etching depth and duty-cycle.

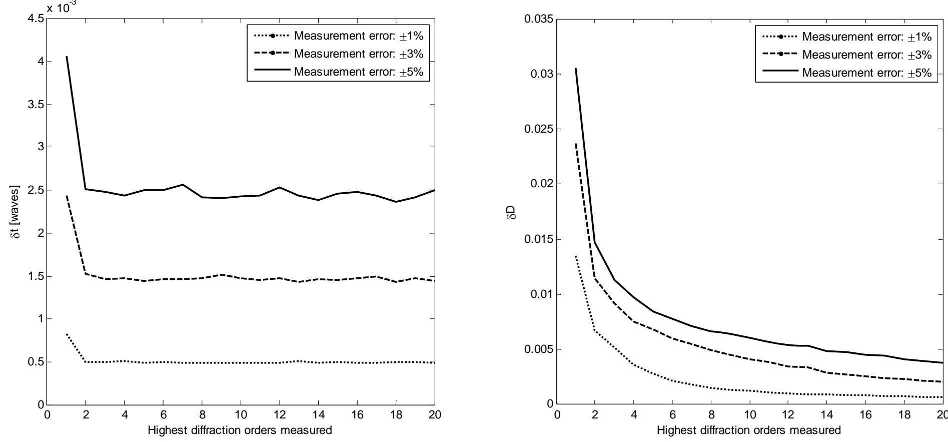

Fig.3 Monte Carlo simulation on etching depth (left) and duty-cycle (right)

The simulation demonstrates that δt does not change significantly by increasing the number of measured diffraction orders. It is proportional to the measurement error. δD decreases with an increase in the number of measured diffraction orders, and finally converges when the number of diffraction orders is sufficiently large. This can be explained by the sensitivity functions of the diffraction efficiencies to the etching depth and duty-cycle $\partial\eta/\partial\phi$, $\partial\eta/\partial D$. Fig.4 shows the sensitivity functions for each diffraction order when the duty-cycle is 0.49, and the etching depth is 0.33λ. The sensitivity of diffraction efficiency to the etching depth drops dramatically at higher diffraction orders, while it oscillates around zero for the duty-cycle. This means the higher diffraction orders do not contribute considerably to the knowledge of the etching depth, so the Monte Carlo simulation gives us a relatively flat curve for δt. However, higher diffraction orders can increase the measurement accuracy of the duty-cycle.

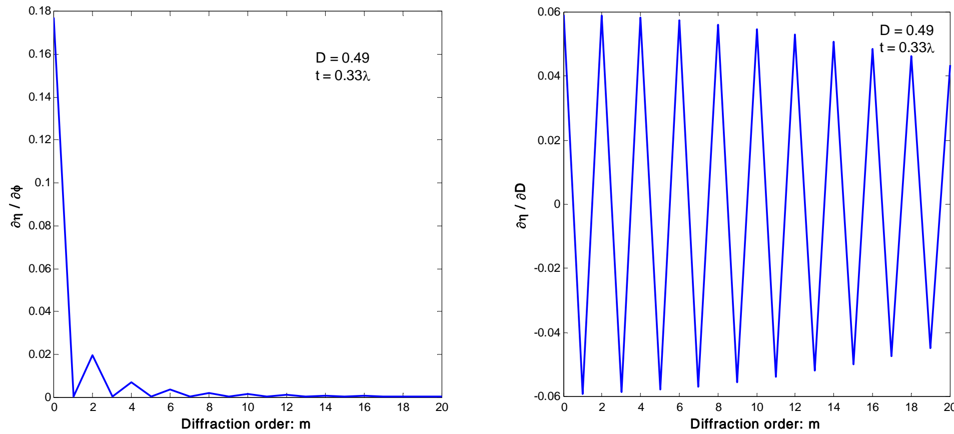

Fig.4 Sensitivity of diffraction efficiencies to etching depth (left) and duty-cycle (right)

By careful measurement, we can control the measurement error within ±1%. In this case, δt and δD are about 0.0005λ and 0.0015 respectively, if we measure up to the $\pm 10^{th}$ diffraction order. These accuracies are sufficient to evaluate the non-uniformities in the duty-cycle and etching depth.

3.3 Amplitude variation measurement

The amplitude of the light from the etched regions can vary due to limitations in the reactive ion etching (RIE) process. The surface roughness of the etched area may vary due to etching, so the light incident on

the CGH scatters differently. By assuming the surface roughness is much smaller than the wavelength of incident light, the coupling of the scattered light to the diffracted light can be ignored. However, the scattering will decrease the amplitude of the diffracted light. This leads to an amplitude ratio variation over the CGH. It is difficult to measure the intensities (or amplitudes) from the etched area and unetched area of the CGH directly. One useful method is to measure the surface roughness of both areas, and then calculate the scattered loss. The scattered loss is zero when the surface is perfectly flat, and it increases with increase in the surface roughness. A simple approximate formula to calculate the total integrated scatter (TIS) for the transmitted light is

$$I_{scat} \approx (2\pi\sigma)^2 = [2\pi(n-1)R_q / \lambda]^2 , \quad (5)$$

where σ^2 is wavefront variance in units of waves, n is the index of refraction of the CGH substrate, and R_q is the RMS surface roughness. The TIS for the reflected light is $I_{scat} = (4\pi R_q / \lambda)^2$. The surface roughness can be measured by an interference microscope. The intensity of the light from the etched and unetched regions can be determined by

$$I \approx 1-(2\pi\sigma)^2 \quad (6)$$

The variation of the surface roughness causes different amount of the scattered loss, which leads to the wavefront errors.

The effect of the surface roughness comes in very slowly. Assume the refractive index of the substrate is 1.5, and the wavelength of interest is 632.8nm. The transmittance of the light at the grating interface is 96% based on the Fresnel formula. If the surface roughness of the etched area is 2nm rms ± 0.5nm rms, the scattered loss would be 0.01% ± 0.005%, and the amplitude variation would be 0.003%. For the above case of 49% duty-cycle and 0.33λ etching depth, the wavefront errors from the surface roughness for the zero and non-zero orders would be -0.0024nm and 0.00086nm, respectively.

4. Error analysis for a phase CGH

The fabrication non-uniformities of a 5-inch phase CGH used for testing an off-axis parabola (OAP) was measured. The CGH was designed with a duty-cycle of 50% and an etching depth of 0.33λ. At 50% duty-cycle, the wavefront sensitivities to etching depth are the same for both the zero order and the first order. Once the first order measurement is subtracted from the zero order one, the wavefront errors from the etching depth can be cancelled. Etching depth of 0.33λ is an optimized parameter that gives good diffraction efficiencies with less wavefront errors from the duty-cycle and amplitude ratio.[13]

The CGH substrate error was measured using the zero order diffraction of the CGH. A 4D Technology PhaseCam 4010 interferometer with an f/7 transmission objective was used. The test setup was similar to that shown in Fig.2. The transmitted wavefront showed 13.6nm rms. Fig.5 shows the measured transmitted wavefront.

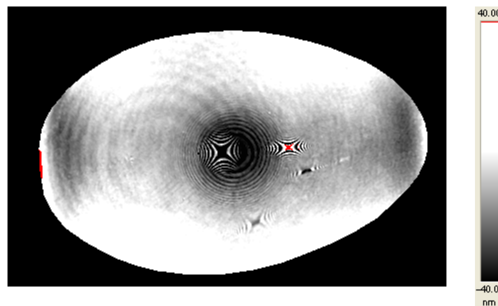

Fig.5 Transmitted wavefront of the CGH substrate

The duty-cycle and etching depth variations were estimated using measured diffraction efficiencies up to the 11th orders. The CGH was illuminated with a 1mm diameter collimated HeNe laser beam. A Newport low-power 918-UV detector and the 2930-C power meter are used to measure the power of each diffraction order. Five points on the CGH are chosen to measure the fabrication non-uniformities. For each power measurement, 500 data points with an interval time of 20ms are averaged by the power meter. The background light is subtracted from each measurement. A non-linear least squares fit is applied to find the duty-cycles and etching depths of these five positions, shown in Table 2. The RMS variations of duty-cycle and etching depth were determined to vary by 0.18% and 0.67%.

Table 2. Duty-cycle and etching depth of the five positions

	D	t (waves)
Point 1	0.4897	0.3274
Point 2	0.4906	0.3315
Point 3	0.4897	0.3317
Point 4	0.4904	0.3326
Point 5	0.4881	0.3275
Average	0.4897	0.33014
RMS variation	0.0009	0.0022
RMS variation in percentage	0.18%	0.67%

The surface roughness of the etched area and unetched area were tested on a WYKO NT-2000 microscope. Table 3 shows that the amplitude variation due to scattering is 0.0033% rms, which is small enough to be neglected.

Table 3. Surface roughness measurement and Strehl ratio calculation

	Unetched area		Etched area		Ratio of amplitudes|A0/A1|
	RMS roughness (nm)	*Iscat*	RMS roughness (nm)	*Iscat*	
Point 1	0.950	0.00002	2.188	0.00012	1.000048
Point 2	1.090	0.00003	1.540	0.00006	1.000015
Point 3	1.110	0.00003	1.840	0.00008	1.000027
Point 4	2.000	0.00010	2.663	0.00017	1.000038
Point 5	1.738	0.00007	2.169	0.00012	1.000021
			Average		1.000030
			RMS variation		0.000033
			RMS variation in percentage		0.000033

The first order wavefront of the CGH is used to test the OAP. Table 4 lists all the wavefront errors from the CGH. The estimated RSS wavefront error of the first order measurement is 13.6nm. Duty-cycle non-uniformities have no impact on the wavefront error for the first order diffraction. Among all the fabrication errors, the substrate error is dominant. To achieve higher measurement accuracy, the substrate errors need to be calibrated.

Table 4. Wavefront errors from CGH fabrication non-uniformities without substrate calibration

Source of Errors	Description	Measured variation	Sensitivities	RMS wavefront Errors at 1st order
CGH substrate	Transmitted wavefront error	13.6 nm	1:1	13.6 nm
Etching depth	Effect on diffracted wavefront	0.67%	$\frac{\partial \Psi_{m=1}}{\partial \phi}$	0.700 nm
Duty-cycle	Effect on diffracted wavefront	0.18%	0	0
Amplitude ratio	Effect on diffracted wavefront	0.0033%	$\frac{\partial \Psi_{m=1}}{\partial (A_0 / A_1)}$	0.001nm
Root-Sum-Squares Error:				**13.6 nm**

The CGH substrate errors can be removed by subtracting the zero order measurement from the OAP wavefront measurement. However, the wavefront errors caused by the fabrication non-uniformities can not be totally removed. With the fabrication errors we measured above, we assessed both the zero order and the first order diffraction wavefronts, and then subtracted one from the other for each error source. Table 5 lists the residual wavefront errors for each error source. The RSS wavefront error drops from 13.6nm to 0.3nm.

Table 5. Wavefront errors from CGH fabrication errors after subtracting the 0th order measurement

Source of Errors	Measured variation	Sensitivities	RMS wavefront Errors
Etching depth error	0.67%	$\frac{\partial \Psi_{m=1}}{\partial \phi} - \frac{\partial \Psi_{m=0}}{\partial \phi}$	0.056 nm
Duty-cycle error	0.18%	$-\frac{\partial \Psi_{m=0}}{\partial D}$	0.300nm
Amplitudes Error	0.0033%	$\frac{\partial \Psi_{m=1}}{\partial (A_0 / A_1)} - \frac{\partial \Psi_{m=0}}{\partial (A_0 / A_1)}$	0.004nm
Root-Sum-Squares Error:			**0.3nm**

Note that the pattern distortion error is not included in the above analysis, because we did not measure the pattern distortion. Assuming the pattern distortion error is 0.1 μm for the 20 μm spacing and the wavelength of interest is 632.8nm, then the wavefront error caused by pattern distortion for the first order is 3.2nm. The pattern distortion becomes the most important error after calibrating the CGH substrate error.

The error analysis of this phase CGH demonstrates that the CGH substrate is the primary error source. The wavefront errors caused by the etching depth, duty-cycle and amplitude are determined to be small enough that we can not measure them using the interferometer. These errors can be neglected in optical testing.

5. Demonstration of substrate calibration

To demonstrate that the substrate error can be calibrated by the zero order wavefront, a custom CGH with 30% duty-cycle and 0.35λ etching depth was fabricated, where the wavelength of interest is 632.8nm. The CGH has a diameter of is 15mm, and generates a spherical wavefront. A reference sphere is used to reflect

the light back for both the zero order and first order measurements. Fig.6 illustrates the setup of the experiment. The first order phase map was subtracted from the zero order one to remove the CGH substrate error. The difference of these two phase maps should record only the fabrication errors in duty-cycle, etching depth, amplitude ratio and pattern distortion. The reference sphere does not introduce any errors in the measurement because it cancels out during the subtraction.

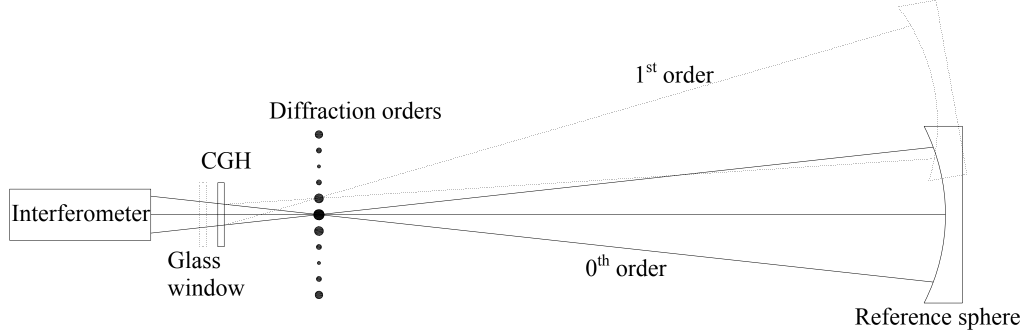

Fig.6 Setup of the CGH substrate calibration

In order to increase the CGH substrate error, a glass window was placed between the interferometer and the CGH, which is equivalent to the CGH substrate error. Table 6 shows measurement results of three configurations with different amount of the equivalent substrate errors. Configuration 1 has no glass window in the setup, while configuration 2 and 3 have different window glasses. Up to about 15nm substrate error is introduced in configuration 3. Tilt, power and astigmatism from the optical test are removed in the measurement, which come from system alignment. For all cases, the difference of the first order and zero order wavefront is about 1nm RMS. The wavefront errors from both fabrication non-uniformities and measurement noises contribute to this difference. This experiment shows that the substrate errors can be removed by subtracting the first order wavefront from the zero order one.

Table 6 Substrate calibration

	RMS error: zero order (nm)	**RMS error: first order (nm)**	**Measured difference (nm)**
Configuration 1	1.677	1.648	0.714
Configuration 2	7.596	7.801	0.779
Configuration 3	16.82	17.43	1.291

6. Conclusions

This paper introduces the parametric model that relates the wavefront performance to the fabrication errors of CGHs, and discusses the methods for determining these fabrication errors. An example of the error analysis for a phase CGH is given by applying this parametric model. This example shows that the substrate error is the dominant error from the CGH, and that it can be removed by subtracting the first order measurement from the zero order one. After performing the substrate calibration, the wavefront errors from the fabrication non-uniformities in duty-cycle, etching depth and amplitude ratio are not significant. This method was applied to an experiment in which several cases of substrate errors were analyzed, where the RMS error is reduced from 17nm to 1nm in the worst case.

Acknowledgements

The authors thank Steven M. Arnold from Diffraction International for fabrication of the CGH. Furthermore, we thank Proteep C.V. Mallik for his help on the experiments.

References:

1. D. Malacara, *Optical Shop Testing,* 2nd ed. (John Wiley & Sons, Inc., 1992)
2. S. M. Arnold, "How to test an asphere with a computer generated hologram", Holographic Optics, Proc. SPIE 1052, 191-197 (1989)
3. H. J. Tiziani, S. Reichelt, etc. "Testing of aspheric surfaces", Lithographic and Micromachining Techniques for Optical Component Fabrication, Proc. SPIE 4440, 109-119 (2001)
4. R. Schreiner, T. Herrmann, J. Röder, S. Müller-Pfeiffer, O. Falkenstörfer, "Design Considerations for Computer Generated Holograms as supplement to Fizeau Interferometers", Proc. SPIE 5965
5. Eugene Curatu and Min Wang, "Tolerancing and testing of CGH aspheric nulls", Proc. SPIE 3782, 581-599 (1999)
6. Y. C. Chang and J. H. Burge "Errors analysis for CGH optical testing," Proc. SPIE 3782, 358-366 (1999)
7. Y.C. Chang, P. Zhou and J. H. Burge "Analysis of Phase Sensitivity for Binary Computer Generated Holograms", Appl. Opt. **45**, 4223-4234 (2006)
8. Fercher, A. F. "Computer-generated holograms for testing optical elements: error analysis and error compensation", Optica Acta, **23**, 347-365 (1976)
9. J. C. Wyant, P. K. O' Neill, and A. J. MacGovern, "Interferometric method of measuring plotter distortion", Appl. Opt. **13**, 1549-1551 (1974)
10. A. Ono and J. C. Wyant, "Plotting errors measurement of CGH using an improved interferometric method", Appl. Opt. **23**, No. 21, 3905-3910 (1984)
11. J. Burge, "A null test for null correctors: error analysis", Proc. SPIE, 1993, 86-97 (1993).